

Micro-Electrode Linked Cyclic Voltammetry Study Reveals Ultra-Fast Discharge and High Ionic Transfer Behavior of LiFePO₄

Yu-Hao Huang^{1,2}, Fu-Ming Wang^{1,3,*}, Tzu-Ting Huang², Jin-Ming Chen², Bing-Joe Hwang⁴
John Rick³

¹ Graduate Institute of Applied Science and Technology, National Taiwan University of Science and Technology, Taipei, Taiwan

² Material Chemical Laboratories, Industrial Technology Research Institute, Hsinchu, Taiwan

³ Sustainable Energy Center, National Taiwan University of Science and Technology, Taipei, Taiwan

⁴ Department of Chemical Engineering, National Taiwan University of Science and Technology, Taipei, Taiwan

*E-mail: mccabe@mail.ntust.edu.tw

Received: 1 December 2011 / Accepted: 29 December 2011 / Published: 1 February 2012

Lithium iron phosphate (LiFePO₄) is a popular cathode material used in lithium ion batteries. However, the ionic transfer mechanism of this compound remains unclear, and requires further investigation. This study employed a micro-electrode analysis technique to examine the ionic transfer characteristics of a single LiFePO₄ particle, formed as an aggregate of many LiFePO₄ primary particles and carbon. This material's electrochemical behavior was then compared with that of a normal composite electrode (fabricated by carbon black and binder). Micro-electrode coupled cyclic voltammetry allows scanning at a rate that is 200 times faster than that attainable with a normal composite electrode. It accurately assesses several electrochemical properties, such as the redox potential and material energy density of LiFePO₄. Furthermore, the Randles-Sevcik equation measures the Li⁺ diffusion coefficient in a single particle more accurately than a normal composite electrode derivative. This calculation yields a one-dimensional (1D) construction, which may have enormous application in the future. The micro-electrode measurement is unique because it reveals the intrinsic original properties of active materials. Therefore, this analysis observation may lead to the development of a highly practical electrode.

Keywords: Lithium ion battery; Single particle; Micro-electrode; LiFePO₄/C; diffusion coefficient

1. INTRODUCTION

Lithium iron phosphate (LiFePO₄) has attracted attention for the last half decade as a potential cathode material due to such advantages as its 1D olivine structure and the presence of Fe that results

in a more powerful performance, a higher energy density, and lower material costs; compared to layer compounds such as LiCoO_2 and $\text{LiNi}_x\text{Mn}_y\text{Co}_z\text{O}_2$. However, LiFePO_4 also has certain drawbacks; these include low ionic electron conductivity, unstable batch quality, and patent monopolization - all of which are limitations that restrict the market for this material [1-3].

Uchida *et al.*, investigated the electrochemical behavior and structure of a single particle of LiMn_2O_4 by using a micro-electrode at 50°C observation. The results indicated that $\text{Li}_{1.1}\text{Cr}_{0.048}\text{Mn}_{1.852}\text{O}_4$ improves cycle performance compared to the original LiMn_2O_4 ; this change occurred at a high temperature due to partial Mn substitution of the excess Li and Cr^{3+} in $\text{Li}_{1.1}\text{Cr}_{0.048}\text{Mn}_{1.852}\text{O}_4$. This technique revealed the intrinsic properties of a single particle during the modification of the material [4-8]. Ceder *et al.*, discovered that LiFePO_4 produces a superior discharge performance, with typical studies conducting 2p chemical binding of phosphate on the surface. According to their simulation, LiFePO_4 offers a 130 mAhg^{-1} at 50 C-rate discharge, and 60 mAhg^{-1} within 600 C-rate, without any decay after 50 cycles [9]. However, Zaghbi *et al.*, (Hydro-Quebec) argue that no experimental evidence exists to support this calculation and challenges Ceder's views on several points [10-15].

In order to purify the electrochemical and intrinsic characteristics regarding cathode and anode material, Dokko *et al.* developed an electrochemical cell for detecting single LiCoO_2 [16] and MCMB [17] particle electrode. According to their results, they found that a single particle of LiCoO_2 can be discharged at 300C and MCMB was released more than 98% of the accommodated Li within 10 sec. These scientific data proved that the material charge transfer process at interface is limited by the binder or other non-conductive materials not the material intrinsic properties.

This study addresses these issues and clarifies the ionic transport properties of LiFePO_4 . We used a modified micro-electrode to aid our research. In addition, we investigated the accuracy of electrochemical measurements relating to both the micro-electrode and the normal composite electrode.

2. METHODS

2.1 Material Synthesis and Electrode Fabrication

LiFePO_4/C was synthesized from a stoichiometric mixture of reagent grade $\text{NH}_4\text{H}_2\text{PO}_4$ (Alfa-Aesar), CH_3COOLi (Aldrich), and $\text{FeC}_2\text{O}_4 \cdot 2\text{H}_2\text{O}$ (Aldrich) according to a traditional solid-state reaction method. The product was ground for twenty min and pressed into pellets, which were heated at 350°C in a quartz-tube furnace with flowing nitrogen gas for six hrs. After slowly cooling to room temperature, the pellets were ground again for twenty min, and a 6 wt % copolymer (guluronic acid) was dissolved in alcohol solution. This mixture was heated to 700°C at a heating rate of approximately 3°C min^{-1} , and left for ten minutes to allow formation of the LiFePO_4/C composite material. After the solid-state reaction, the carbon content of the LiFePO_4/C powder was measured by elemental analysis (EA).

Electrochemical characterization was performed using a CR2032 coin-type cell. The composite

cathode consisted of 89 wt % active material (LiFePO_4/C), 4 wt % graphite powder KS-4 (Timcal), 2 wt % Super P (Timcal), and a binder of 5 wt % polyvinylidene fluoride [(PVDF) Kureha]. This composite slurry was coated onto the aluminum foil current collectors (Nippon foil) and dried for five min at 120°C in air, followed by twelve hrs in a vacuum oven at 90°C .

The calculated electrode density, determined from the total mass of the composite electrode, was found to be 0.9 g cm^{-3} . A circle with a diameter of approximately 13 mm was punched out of the electrode. The assembly of half-cells in a CR2032 coin-type cell was performed in the dry room. The electrolyte was 1M LiPF_6 (Kishda) dissolved in a mixture of solvents, namely ethylene carbonate (EC) (Alfa-Aesar), propylene carbonate (PC) (Alfa-Aesar), dimethyl carbonate (DMC), (Alfa-Aesar) and ethylmethyl carbonate (EMC) (Alfa-Aesar). The volume ratio of these solvents was 3:1:4:2, respectively. Due to the boiling point of electrolyte being low, we minimized the risk of evaporation by conducting our experiment in a glove box with an external port to avoid changes in the electrolyte composition during the measurements.

2.2 Microelectrode analysis procedure

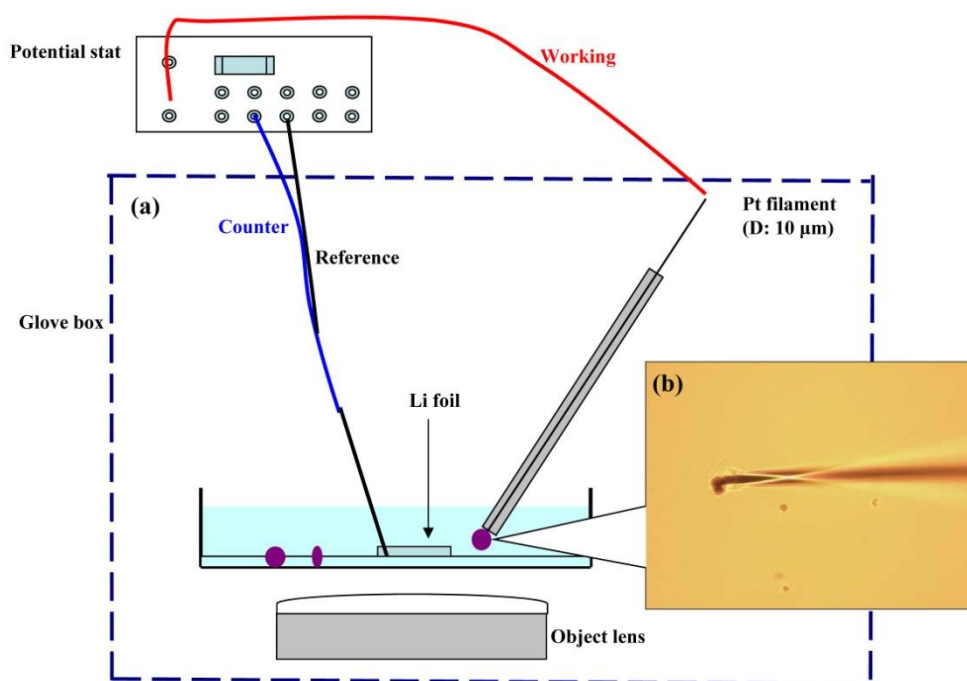


Figure 1. a) Schematics illustration of the microelectrode measurement system and b) OM of microelectrode touched single particle

A single particle, which is an aggregated particle of many LiFePO_4 primary particles and carbon, was fixed in a Petri dish. The dish bottom was spun and coated with a PVDF layer $3\text{ }\mu\text{m}$ thick. The PVDF layer was manufactured by mixing a typical weight ratio of (N-Methyl-2-pyrrolidone (NMP): PVDF = 95:5) binder solution. A small quantity of the binder solution (0.2 g) was dropped

into a Petri dish central and spun at 1000 rpm for 20 seconds to form a uniform PVDF layer. The particle was sprayed by inert gas from the capillary onto the PVDF layer, and a homogenous sample was obtained by a vacuum process at 120°C for 1hr. Optical microscopic examination showed the thickness of the binder layer after heat treatment to be about 4-8µm. Figure 1 shows the micro-electrode system, manufactured with a 10 µm diameter platinum filament (Nilaco), welded by enamel-insulated wire with a heat-shrinkable capillary tip (Word precision instrument), and a grinding electrode tip.

2.3 Electrochemical measurements

We compared the measurements taken of a single particle by micro-electrode analysis with those of a composite electrode. A composite electrode was assembled in a coin cell, and its electrochemical properties were evaluated. The electrochemical measurements were made using a potentiostat/galvanostat (HEKA-PG340 & CHI-608d), the charge-discharge range being 2.0-4.0 V. The Randles-Sevcik equation, shown in Eq. 1, was used to calculate a diffusion coefficient. This entailed plotting the peak current (i_p) and the square root of the scan rate ($v^{1/2}$) for the micro-electrode and the composite electrode.

$$i_p = 2.69 \times 10^5 n^{3/2} A D^{1/2} C^* v^{1/2} \quad (1)$$

where i_p is the peak current in amperes, F is the Faraday constant, C^* is the initial concentration in molcm⁻³, v is scan rate in Vs⁻¹, A is electrode area in cm², and D is the diffusion constant in cm²s⁻¹.

3. RESULTS AND DISCUSSION

3.1 Material identification of LiFePO₄

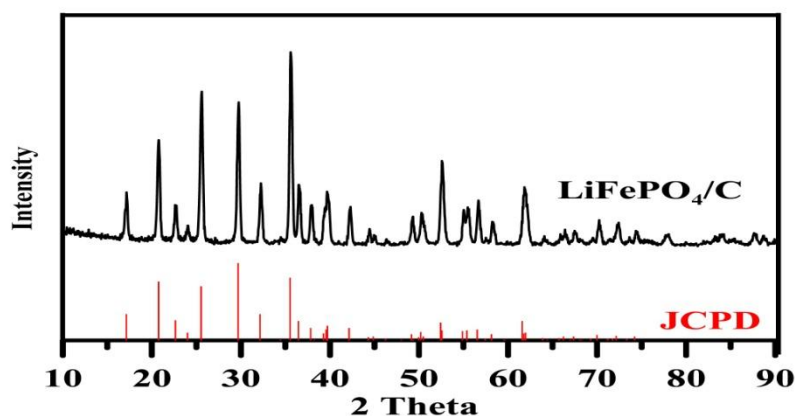


Figure 2. XRD spectra of LiFePO₄/C

The LiFePO_4/C was analyzed for phase and purity by X-ray diffraction (XRD) using a Philips PW3710 diffractometer with Cu K_α radiation (wavelength = 1.54 \AA). Figure 2 shows the XRD pattern of the LiFePO_4/C powders. This pattern is similar to an orthorhombic system in the $Pnma$ space group (JCPDS card No.81-1137). No crystalline carbon diffraction peak (002) was detected, indicating that the residual carbon was amorphous and overlapped the crystalline carbon peak of LiFePO_4 (111). According to previous studies, impurities can cause a decrease in ionic conductivity, capacity, and cycling rates [18-20]. After carbon coating, the olivine structure of the LiFePO_4/C was maintained, suggesting that impurities caused by iron reduction during the carbon coating process were eliminated.

3.2 Cyclic voltammetry analysis

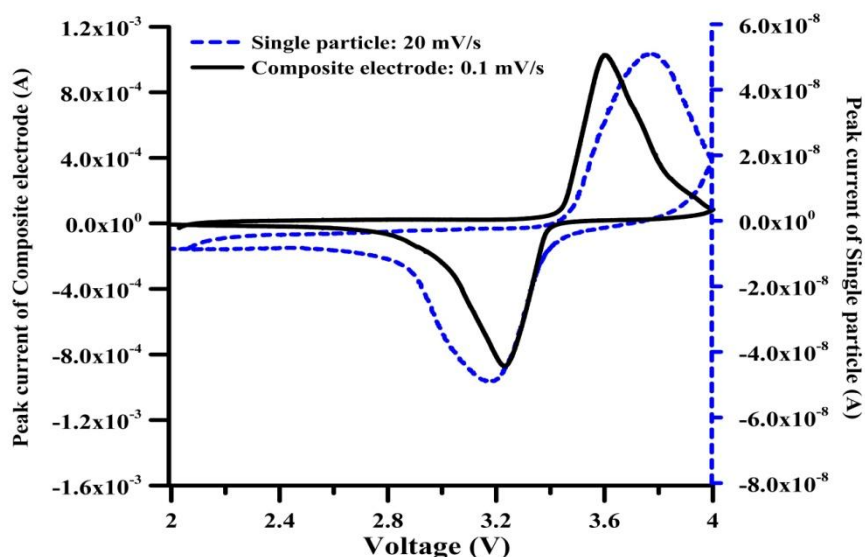


Figure 3. Cyclic voltammogram for LiFePO_4/C (dashed line: single particle at scan rate of 20 mVs^{-1} , and solid line: composite electrode at scan rate of 0.1 mVs^{-1})

Figure 3 shows the cyclic voltammetry scans from the micro-electrode and the composite electrode at two different scanning rates, namely 20 mV/s (dashed line) and 0.1 mV/s (solid line). For the composite electrode, the oxidation and reduction potentials of LiFePO_4/C were 3.65 V ($I_{p_a} = 1.13 \times 10^{-3} \text{ A}$) and 3.25 V ($I_{p_c} = -8.32 \times 10^{-4} \text{ A}$), which is in good accord with previous research [21]. However, the micro-electrode observation of a LiFePO_4 single particle revealed a slight shift in the redox couple to 3.8 V ($I_{p_a} = 5.21 \times 10^{-8} \text{ A}$) and 3.2 V ($I_{p_c} = -4.98 \times 10^{-8} \text{ A}$). The composite electrode showed enhanced electrochemical (EC) properties. One reason for this is that mixing LiFePO_4 with a binder and carbon black enhances electron conductivity and eliminates ohmic polarization during the electrochemical reaction. In addition, the contact resistance barrier of the micro-electrode with LiFePO_4 may cause polarization, thus leading to redox changes within the material.

Figure 3 shows the behavior of EC as measured by either a micro-electrode or a composite electrode, with the micro-electrode scanning rate being 200 times faster. The redox potential is clearly illustrated and shows that the micro-electrode provides approximately the same proportional current

density response and equilibrium voltage plateau at 3.4 V when compared to the composite electrode. We concluded that the high scanning frequency micro-electrode provides accurate measurements, and can be accurately used to detect reaction potentials.

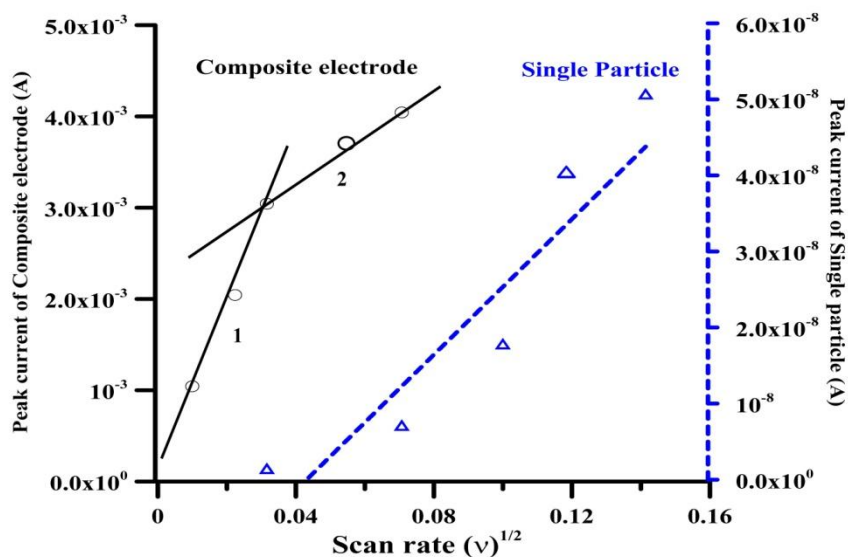


Figure 4. Cyclic voltammetry of single particle and composite electrode to derive lithium chemical diffusion coefficient. The relationship of the peak current (i_p) and square root of scan rate ($v^{1/2}$)

Table 1. Lithium ion diffusion coefficient derived of cyclic voltammetry of single particle and composite electrode

| Composite electrode (cm ² s ⁻¹) | | Single particle (cm ² s ⁻¹) |
|--|------------------------|--|
| D ₁ | D ₂ | D |
| 6.61*10 ⁻¹⁴ | 5.10*10 ⁻¹⁵ | 4.96*10 ⁻¹⁴ |

To describe the Li ion’s diffusion behavior in the context of either a single particle or the composite LiFePO₄ electrode, the Randles-Sevcik equation was used. We estimated the diffusion coefficient by plotting the scan rate verse the cathodic peak current. A single slope resulted for the single particle, with a value of $4.96 \times 10^{-14} \text{ cm}^2\text{s}^{-1}$ (on the section of the dashed line). However, the solid line of the composite electrode showed two slopes rather than a linear slope, as shown in Figure 4. Table 1 shows that the first and second sections were approximately 6.61×10^{-14} and $5.1 \times 10^{-15} \text{ cm}^2\text{s}^{-1}$, respectively; this result is due to the semi-infinite linear diffusion at the electrode/interface from the bulk solution. The binder and conductive carbon effects introduce an additional kinetic bottleneck because the binder additives in the electrode cause the electrons to move slowly through the electrode. This causes a perceptible time lag between the potential at the voltage source and that at the electrode/solution interface. Thus, the diffusion coefficient of a single particle is unchanged and is higher than that of the composite electrode. This becomes apparent at the high scanning rate and

highlights the limitations of lithium iron phosphate. Our findings regarding the diffusion behavior of lithium iron phosphate were essentially the same as those obtained by Ceder and other researchers [9, 22].

3.3 Rate capability of LiFePO_4/C

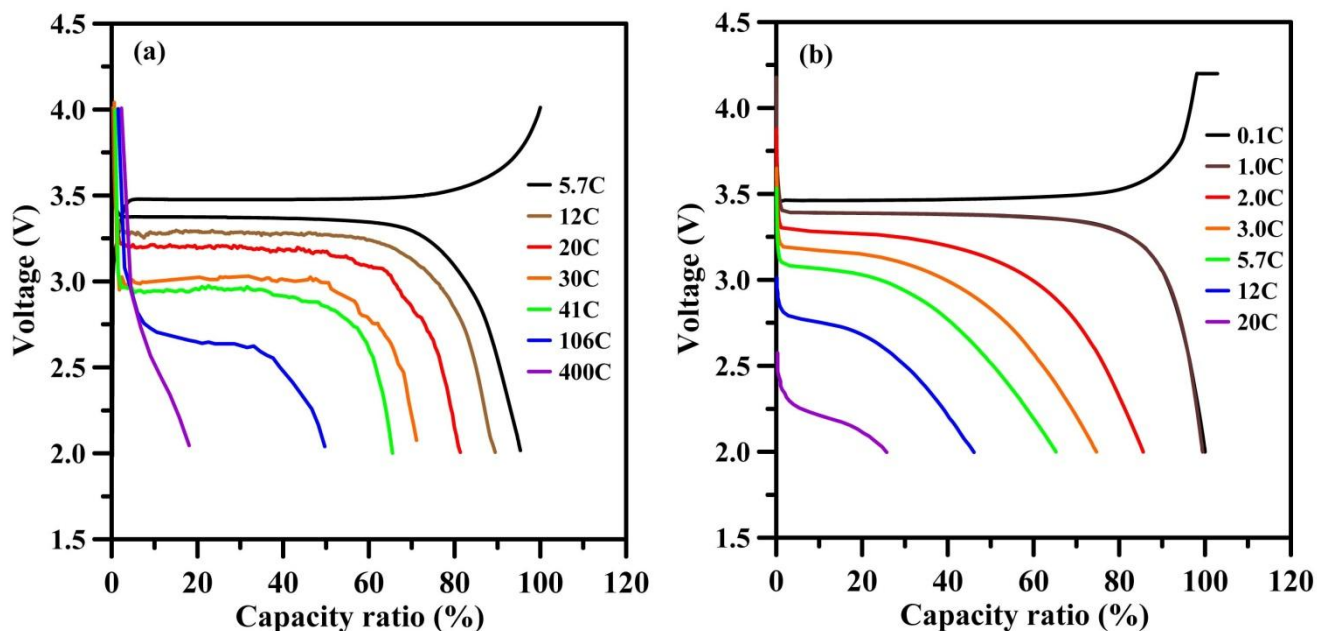


Figure 5. Discharge curves of a) single LiFePO_4/C particle and b) composite electrode LiFePO_4/C at different C rates.

Figure 5 illustrates the C-rate capability of a single LiFePO_4 particle (15 μm diameter) with a theoretical capacity of 1.08×10^{-6} mAh, under 2 nA (5.7 C) charge and 2-30 nA (5.7-400C) discharge currents. Figure 5a presents our finding that the single LiFePO_4/C particle can be directly discharged at the high rate of 5.7 C, while retaining an excellent power density of 95 % capacity ratio with a 3.4 V working potential. When the discharge rate was increased to 106 C, the material maintained 50 % of its original capacity with an average potential of 2.7 V. In contrast, the composite electrode showed a poor performance, as illustrated in Figure 5b, resulting from the adhesion agent impeding ionic conduction. The composite electrode possesses an effective discharge rate of 5.7 C, which retains only 65 % of its capacity.

Our research demonstrates the natural properties of LiFePO_4 . However, several reasons may cause the composite electrode not to achieve its high power potential, such as current collector thickness, the roller compaction density of the electrode, and internal battery resistance. These factors limit the high ionic transfer capacity of the material. In addition, Uchida *et al.*, compared the three-dimensional (3D) spinel structure of lithium manganese oxide (LiMn_2O_4), as measured with the micro-electrode, and showed that the 1D structure of olivine yields excellent ion transmission [8]. Our electrochemical experiments have proved that intercalation and de-intercalation of the ionic channel

must be fixed to a unitary direction, i.e. not a 3D channel, and that a material with superior natural electronic conductivity can enhance ultimate battery performance.

4. CONCLUSION

The micro-electrode has shown itself to be a powerful measurement tool, able to be employed for accurate electrochemical testing that is capable of revealing critical properties of a single particle. Comparative cyclic voltammetry indicated that cation diffusion in the single particle material is dramatically higher than in an analogous composite electrode battery. This suggests that the binder and inhomogeneous carbon black dispersion significantly lower the composite material's natural performance. Our research verified that LiFePO_4/C shows an excellent and unique 1D superior ionic diffusion. In addition, we demonstrated the utility of micro-electrodes for validating measurements in industrial applications; either to clarify a material's electrochemical properties, or as a tool to rapidly evaluate its commercial viability.

ACKNOWLEDGEMENT

This research is supported by the Ministry of Economic Affairs, R.O.C (No.8354DA1510). The authors are also grateful for the financial support from the National Science Council of Taiwan, R.O.C, under Grant NSC 100-2923-E-011-001-MY3 and NSC 100-3113-E-011-002.

References

1. A.K. Padhi, K. S. Nanjundaswamy, J. B. Goodenough, *J. Electrochem. Soc.* 144 (1997) 1188.
2. A.K. Padhi, K.S. Nanjundaswamy, C. Masquelier, S. Okada, and J. B. Goodenough, *J. Electrochem. Soc.* 144 (1997) 1609.
3. M. Thackeray, *Nat. Mater.* 1 (2002) 81.
4. K. Dokko, S. Horikoshi, T. Itoh, M. Nishizawa, M. Mohamedi, I. Uchida, *J. Power Sources* 90 (2000) 109.
5. I.Uchida, M. Mohamedi, K. Dokko, M. Nishizawa, T. Itoh, M. Umeda, *J. Power Sources* 97-98 (2001) 518.
6. M. Nishizawa, I. Uchida, *Electrochim. Acta* 44 (1999) 3629.
7. K. Dokko, M. Mohamedi, Y. Fujita, T. Itoh, M. Nishizawa, M. Umeda, I. Uchida, *J. Electrochem. Soc.* 148 (2001) A422.
8. I.Uchida, H. Fujiyoshi, S.Waki, *J. Power Sources* 68 (1997) 139.
9. B. Kang, G. Ceder, *Nature* 458 (2009) 190.
10. K. Zaghbi, J. B. Goodenough, A. Mauger, C. Julien, *J. Power Sources* 194 (2009) 1021.
11. N. Ravet, Y. Chouinard, J. F. Magnan, S. Besner, M. Gauthier, M. Armand, *J. Power Sources* 97-98(2001) 503.
12. P. Axmann, C. Stinner, M. Wohlfahrt-Mehrens, A. Mauger, F. Gendron, C. M. Julien, *Chem. Mater.* 21 (2009) 1936.
13. K. Zaghbi, A. Mauger, F. Gendron, C. M. Julien, *Chem. Mater.* 20 (2008) 462.
14. P. Prosini, M. Lisi, D. Zane, M. Pasquali, *Solid State Ionics* 148 (2002) 45.
15. C. V. Ramana, A. Mauger, F. Gendron, C. M. Julien, K. Zaghbi, *J. Power Sources* 187 (2009) 555.
16. K. Dokko, N. Nakata, K. Kanamura, *J. Power Sources* 189 (2009) 783.

17. K. Dokko, N. Nakata, Y. Suzuki, K. Kanamura, *J. Phys. Chem. C* 114 (2010) 8646.
18. J. Liu, R. Jiang, X. Wang, T. Huang, A. Yu, *J. Power Sources* 194 (2009) 536.
19. J. Ni, M. Morishita, Y. Kawabe, M. Watada, N. Takeichi, T. Sakai, *J. Power Sources* 195 (2010) 2877.
20. F. Teng, S. Santhanagopalan, R. Lemmens, X. Geng, P. Patel, D. D. Meng, *Solid State Sciences* 12 (2010) 952.
21. D. Y. W. Yu, C. Fietzek, W. Weydanz, K. Donoue, T. Inoue, H. Kurokawa, and S. Fujitani, *J. Electrochem. Soc.* 154 (2007) A253.
22. G. Ceder, B. Kang, *J. Power Sources* 194 (2009) 1024.